

SYNTHESIS AND CHARACTERIZATION OF COBALT DOPED ANTIMONY SULFIDE THIN FILMS FOR SOLAR ENERGY APPLICATIONS

Zainab Zishan¹, Sara Yaseen², Abdul Ghafar Wattoo^{*3}, Uzair Ahmad⁴, Misbah Aurangzeb⁵
Mustansar Nadeem⁵, Aurang Zeb^{*6}

^{1,2, *3}Institute of Physics, Khwaja Fareed University of Engineering and Information Technology, Rahim Yar Khan-64200, Pakistan

⁴Department of Physics, University of Gujrat, Gujrat, Pakistan

^{5, *6}Department of Physics, Federal Urdu University of Arts, Sciences and Technology, Islamabad-56000, Pakistan

DOI: <https://doi.org/10.5281/zenodo.19882686>

Keywords

Antimony sulfide, Solar cells, Chemical bath deposition, thin films.

Article History

Received: 28 January 2025

Accepted: 13 March 2025

Published: 27 March 2025

Copyright @Author

Corresponding Author: *

Abdul Ghafar Wattoo

Aurang Zeb

Abstract

Here in this research, we have prepared Cobalt-doped antimony sulfide thin films using Chemical Bath Deposition (CBD) method on the glass substrate and analyzed the impact of concentration on physical properties of prepared thin films by annealing them at 250 °C for two hours. Structural analysis from X-ray diffraction (XRD) revealed that the films were polycrystalline in nature with orthorhombic phase and its crystallite size decrease from 19 to 10 nm. Scanning electron microscopy (SEM) showed surface morphology and grain growth of prepared thin film which were improved with increasing cobalt concentration. Raman vibration mode confirmed the presence of the antimony sulfide phase in the prepared thin films and showed that their Raman spectra are unevenly dominated by stretching vibration modes $\nu(\text{Sb-S})$. The annealed Sb_2S_3 thin films exhibited energy band gap values of 0.56 - 0.95 eV. The pure and Co-doped antimony sulfide thin films showed high absorption coefficient of about 10^4 cm^{-1} indicating Co-doped antimony sulfide thin films are suitable for solar cell applications.

1. Introduction

Chalcogenide thin films have attained much attention due to its excellent optoelectronic photovoltaic, and thermoelectric applications [1, 2]. Antimony sulfide thin film is an attractive solar absorber material that has garnered tremendous interest because of its fascinating properties for solar cells including suitable band gap (1.78–2.50 eV), high absorption coefficient (10^4 cm^{-1}), excellent stability and earth abundance [3]. It has high values for index of refraction with high valued absorption coefficient of about 10^5 cm^{-1} [4][5, 6] and have well-distributed quantum size effects these are some of its properties which made it suitable for

solar cell applications [7]. Antimony tri-sulfide (Sb_2S_3) thin films observed to have complication due to its high values of resistance and found to have low transmittance, which somehow hold back its large scale applications [8]. Photovoltaic devices have been developed to boost the usage of solar energy. Silicon solar cells during past years proved as the most competent materials but due to their high production cost they cannot overcome the existing energy crisis [9]. The material's structural, electrical and optical properties should be observed which verify it as promising candidate for solar cell applications. It is observed from the recent literature surveys that the properties of material can be enhanced

by two ways; first one is by varying deposition method which also affects its production cost and second one is by adding different dopants which somehow boost up its optical and electrical properties.

Antimony sulfide thin films were deposited by using several techniques like simple and cost effective chemical bath deposition method [10], spray pyrolysis [11], spray pyrolysis [12], dip and dry method [13] and vacuum thermal technique [14]. Various dopants were used to enhance the physical properties of material such as phosphorous, carbon, bismuth etc.[15, 16]. The optical properties can also be enhanced by increasing the films deposition time and by annealing the deposited films which also made them crystalline [16]. Due to its vast area deposition, low-cost and low temperature chemical bath deposition has widely been used. Various researches have been made in this context by deposition of Sb_2S_3 thin films using CBD [17-19]. The band gap values of thin films change by varying its deposition techniques. As Savadogo and Mondal measured 1.8 eV band gap energy for Sb_2S_3 thin films by using CBD [20]. Bhosale et al, measured band gap energy 1.55 eV by using spray pyrolysis method [4]. Later, Yesugade et al. prepared Sb_2S_3 , As_2S_3 , and Bi_2S_3 thin films by using Electro Deposition Technique and observed 1.7 eV band gap energy of Sb_2S_3 [21].

Earlier, it was observed that absorption of antimony sulfide thin films enhanced by doping. Ma et al, showed that the absorption of Sb_2S_3 thin films was increased by doping it with titanium which also improves the device current density which leads higher efficiency [22, 23]. In this study, we have prepared Co-doped antimony sulfide Sb_2S_3 thin films by varying

cobalt concentrations of 1%, 2%, 3% and 4% by CBD method optimized at the temperature of about 10 °C. The physical and morphological characteristics of undoped and cobalt doped antimony sulfide thin films were analyzed by various techniques of characterization i.e., UV/Visible spectroscopy, scanning electron microscopy and X-ray diffraction. The energy gap for cobalt doped antimony sulfide films was found to 0.56-0.95 eV. Higher values of the absorption coefficient represent potential of the prepared thin films as good solar absorbers.

2. Experimental Details

Pure and cobalt-doped antimony sulfide Sb_2S_3 thin films were deposited onto microcrystalline glass substrate. The whole apparatus was thoroughly cleaned with acetone and distilled water and then dried. These films were fabricated by placing these thoroughly cleaned glass slides vertically in the solution by chemical bath deposition technique. The solution of pure and cobalt doped antimony sulfide thin films were prepared by the addition of 650 mg antimony chloride SbCl_3 (Merck, 99%) well dissolved in 10 ml of acetone CH_3COCH_3 (Merck, 99%) with 65 ml distilled water and 25 ml of 1M sodium thiosulphate $\text{Na}_2\text{S}_2\text{O}_3$ (Aldrich, 99%). After the solution color turned to orange-yellow then 1%, 2%, 3% and 4% CoCl_2 was added in the solution which turned its color to dark orange when stirred for 10-15 minutes on hot plate. The low bath temperature was maintained for about 4 hours. Then the films prepared were annealed at 250 °C for 2 hours under vacuum to enhance their crystallinity. The apparatus set up for CBD is shown in Fig. 1.

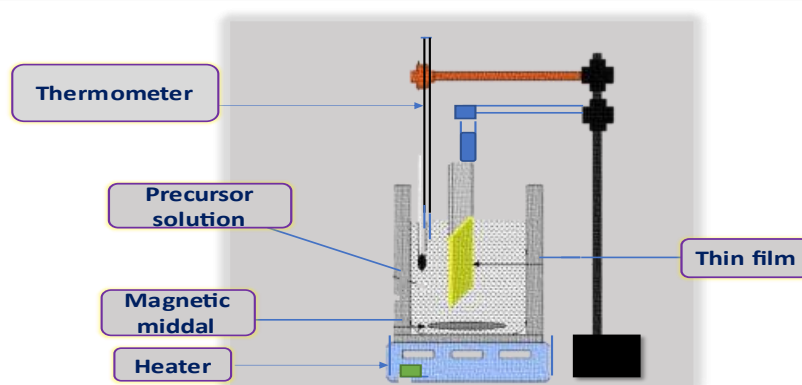


Figure 1. Experimental set up of CBD technique.

2.2. Characterization techniques

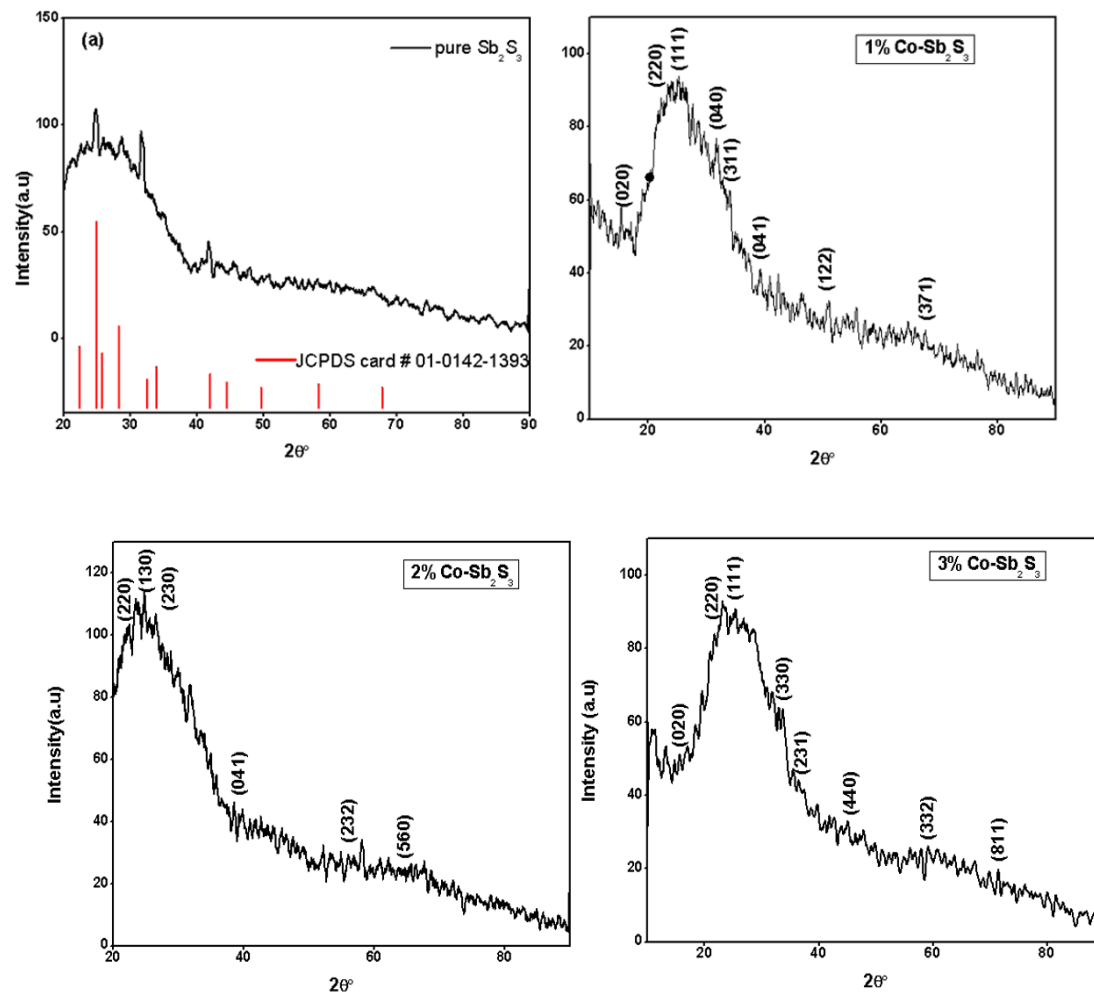
Thin films prepared by CBD technique were characterized by Raman spectroscopy and XRD (X-ray diffraction technique to study crystal and their structural properties). The XRD results showed the pattern of Co-doped Sb_2S_3 thin films which were achieved by $\text{K}\alpha$ radiation with 1.542 Å wavelength. The morphological characteristics of undoped and cobalt doped antimony sulfide thin films were detected by SEM. UV/Vis Spectrometer was used to measure the optical properties like transmission, energy gap and absorption coefficient etc. of the films in the range of 400-900 nm.

3. Results and Discussions

3.1 X-Ray Diffraction (XRD) analysis

The XRD plots of prepared films matched with standard pattern of Sb_2S_3 with JCPDS card # 01-0142-1393 which can be seen in Fig. 2(a). The XRD plot of undoped and Co-doped Sb_2S_3 thin films with varying cobalt concentrations is shown in Fig. 2(b). It was observed that the films were poly crystalline, well deposited and adhesive. The XRD results showed the crystallinity of thin films in 2θ range of 20° - 90° . The change in peak positions towards lower angle is due to the difference in ionic radii of Sb^{+3} (0.90 Å) and Co^{+2} (0.65 Å) which resulted in distortion in the lattice. This distortion in the lattice is also evident from the increase in lattice

parameters, hence lattice was expanded. On further increasing the dopant concentration, diffraction peaks are broadened and correspond to amorphous nature, as shown in Fig. 2 (d, e) leading to poor crystallinity. The replacement of Sb^{+3} having ionic radius of 0.90 Å with Co^{+2} having ionic radius of 0.65 Å induces stress in the crystal and may cause dislocation of the atoms. This fact is obvious as the dislocation density increases with increasing dopant concentration. These XRD plots displayed a slight increase in full width half maximum (FWHM) which might be due to decrease in thickness of thin films and no further distinctive peaks of cobalt were observed which confirmed the crystallinity of the antimony sulphide thin films with increasing cobalt concentrations similar peaks were observed previously [24]. The structural parameters such as crystallite size, dislocation density and lattice parameters were calculated by XRD pattern in Fig 2. These calculated structural parameters are shown in Table I, which shows reduction in crystallite size, increase in dislocation density with varying cobalt concentrations. The researchers such as [25-27] revealed the corresponding results. It can be observed that the films have identified peaks which are well-equivalent with standard patterns showed enhancement in crystallinity of deposited films.



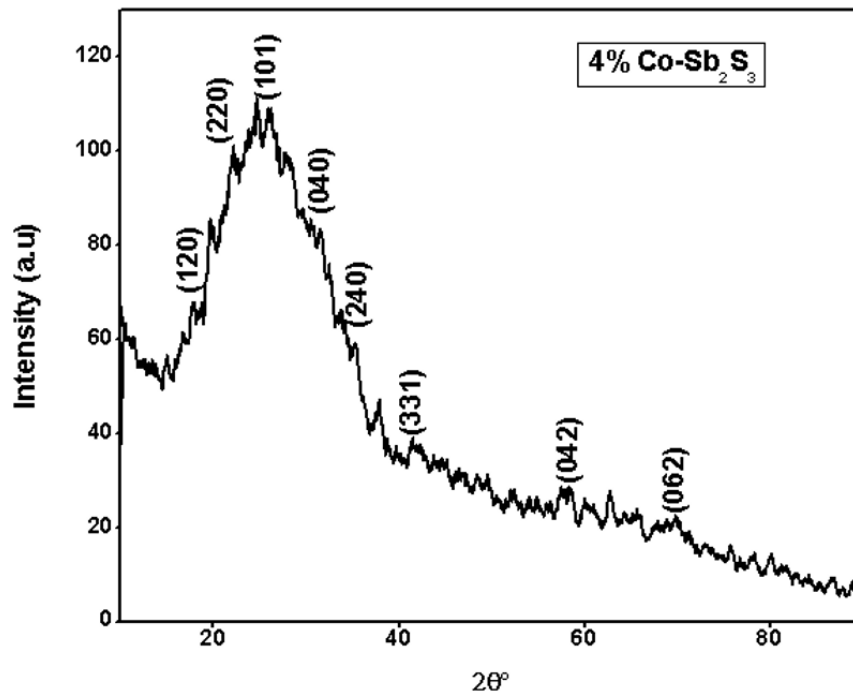


Figure 2. XRD pattern of Co-doped Sb_2S_3 thin films.

The structural parameters such as crystallite size, dislocation density and lattice parameters etc., for cobalt doped and undoped Sb_2S_3 thin films calculated by plots of XRD to obtain its microstructure characteristics. The grain size $\langle D \rangle$ is calculated by Scherrer's equations:

$$D = \frac{K\lambda}{\beta \cos \theta} \quad (1)$$

where $\lambda = 1.542 \text{ \AA}$ is the X-ray wavelength, β gives FWHM from Fig. 2, the k is the constant have value of 0.9 and θ gives the Bragg's angle from XRD plot.

The lattice constants which is "a", "b", and "c", were estimated by the relation below [28]:

$$\frac{1}{d^2} = \frac{h^2}{a^2} + \frac{k}{b^2} + \frac{l^2}{c^2} \quad (2)$$

The dislocation density (δ) and lattice strain (ϵ) for pure and cobalt doped antimony sulfide thin films was estimated by:

$$\delta = \frac{1}{D^2} \quad (3)$$

$$\epsilon = \frac{\beta}{\tan \theta} \quad (4)$$

Whereas, X-ray density (ρ) and unit cell volume (V) was estimated by:

$$V_{\text{cell}} = \frac{abc}{ZM} \quad (5)$$

$$\rho = \frac{ZM}{N_A V_{\text{cell}}} \quad (6)$$

where N_A is the Avogadro number, Z is the number of molecules in formula unit, M is the molar mass. The calculated above mentioned structural parameters can be seen in Table I.

Crystallite size observed to be decrease from 19 nm to 10 nm with increasing cobalt concentrations. It showed crystallinity of Sb_2S_3

thin films. While dislocation density increased from $2.7 \times 10^{-3} \text{ nm}^{-2}$ to $11.2 \times 10^{-3} \text{ nm}^{-2}$ which shows the increment of deformation in the crystal, caused due to defects produced by doping. Lattice strain also reduced from 2.52 to 4.22, results in the decrease of crystallite size with increasing cobalt concentrations.

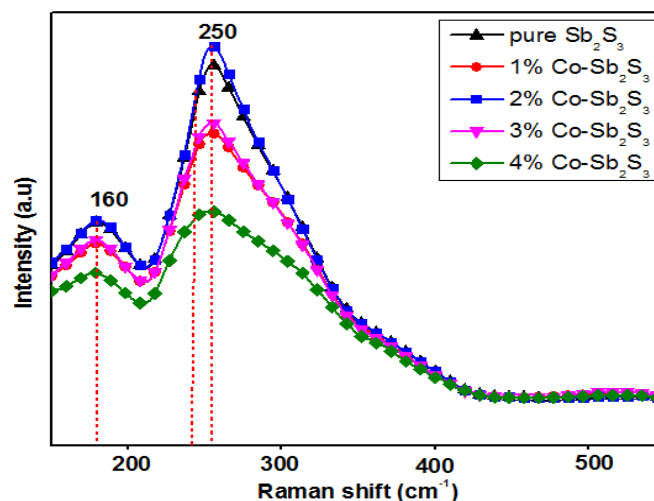
Table I. Microstructural parameters for pure and Co-doped Sb_2S_3 thin films from XRD patterns.

Parameters	1%	2%	3%	4%
a (Å)	11.25	11.22	11.23	11.25
b (Å)	11.33	11.31	11.313	11.33
c (Å)	3.83	3.84	3.841	3.83
$V_{\text{cell}}(\text{Å})^3$	488.18	487.55	488.38	488.18
ρ (g/cm^3)	3.72	3.73	3.72	3.728
D (nm)	19	13	11	10
δ (nm^2)	2.7×10^{-3}	5.9×10^{-3}	8.2×10^{-3}	11.2×10^{-3}
ε	2.52	2.86	3.39	4.22

3.2 Raman spectroscopy:

The prepared thin films were analyzed by raman spectroscopy which gives the details of vibrational modes in solids. The raman spectral region for pure and cobalt doped Sb_2S_3 thin films shown in Fig. 3 ranges from 200 cm^{-1} - 500 cm^{-1} [29]. The broad raman band for pure Sb_2S_3

film is positioned at 250 cm^{-1} with high intensity which then decreased by increasing cobalt concentrations also reported in literature earlier which shows the crystalline nature of pure and cobalt doped Sb_2S_3 thin films [30]. The raman spectra in Fig. 3 showed only two modes of vibrations i.e., Sb-Sb and Sb-S.

Figure 3. Raman spectra of pure and cobalt doped Sb_2S_3 thin films.

3.3 Scanning electron microscopy (SEM) results

The SEM micrographs of pure and cobalt-doped antimony sulphide thin films with different cobalt concentrations of 1%, 2%, 3% and 4% are shown in Fig. 4. The given SEM micrographs showed varying grain size upon addition of cobalt. The pure antimony sulphide thin films showed well deposition of solid grains with diameter of about $107 \mu\text{m}$. The SEM micrographs in Fig. 4(a) indicates the irregular distribution of excessive growth of particles on the surface Sb_2S_3 samples which was also observed in recent studies of Sb_2S_3 thin films by

CBD [31] It can be seen in Fig. 4(b) the uneven distribution of irregular growth of spherical particles on the sample of Sb_2S_3 thin films which was also observed earlier in the literature in the preparation of Sb_2S_3 thin films with CBD method [28]. The cobalt-doped Sb_2S_3 thin films are evenly distributed and the particles are agglomerated upon increasing cobalt concentration that is reported to be common in chemical bath deposited Sb_2S_3 films. The incorporation of cobalt in Sb_2S_3 thin films observed to increase the homogeneity of thin films with decreasing number of surface particles as well as slight increase in film thickness. These

results may be caused by the generation of new nucleation centers due to Co-doping^[32]. It showed the variation in the nature and size of grains upon addition of increasing Co-concentrations. We have an idea that Sulphur placement may be filled by cobalt in Sb_2S_3 films which increase its lattice volume. The particles are found to be dense at higher Co concentrations which leads to the firmness of

films and reduction in surface unevenness. The grain size estimated to be 94 μm , 92 μm , 90 μm and 87 μm for varying cobalt concentrations 1%, 2%, 3% and 4% Co-doped Sb_2S_3 thin films respectively, which showed compactness of thin films [33]. The SEM micrographs confirmed the reduction in inter-particle distances with increasing cobalt concentrations in antimony sulphide films [34].

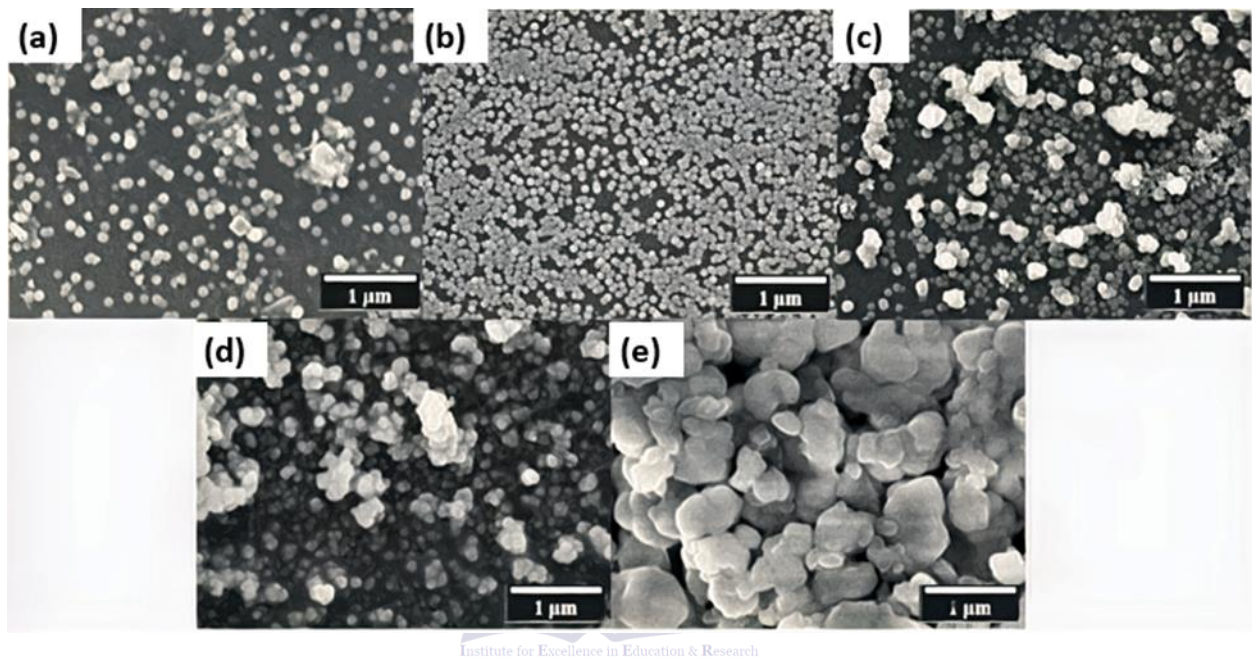


Figure 4. Scanning electron micrographs for pure Sb_2S_3 and varying Co concentration

(a) Sb_2S_3 (b) 1%, (c) 2%, (d) 3% and (e) 4%

3.4 UV-visible spectroscopy results

The cobalt doped Sb_2S_3 thin films prepared by CBD method were characterized by UV/Visible spectroscopy which gives information about their optical constants such as absorbance, transmittance band gap etc. The UV-plot of pure and Co-doped Sb_2S_3 thin films for absorbance are shown in Fig. 5(a). It can be seen that the absorption plot ranges from 400 nm-900 nm. Thin film shows maximum absorbance in the

$$T = 2 - \log A$$

Where A is the absorbance. The transmittance spectra of pure and 1% Co-doped Sb_2S_3 thin films are shown in Fig. 5(b) which shows low transmittance of about 40%. It can be seen that 2%, 3% and 4% cobalt-doped films have high transmittance of about 45%, 50% and 60 % respectively in visible region as compared to 40% transmittance of pure and 1% Co-doped

range of 500 nm-700 nm in the visible region. The λ_{max} for pure and 1% Co-doped Sb_2S_3 thin films is at 500 nm while that for 2%, 3% and 4% is below 400 nm. This increased absorbance lead to decreased transmittance in visible region supports that these films will be used as an absorber layer and produce high values of current [10].

As UV-visible spectroscopy measures absorbance so transmittance is calculated by [35]:

$$(7)$$

Sb_2S_3 thin films in Fig.5(b). These transmittance spectra revealed that transmittance increases with the increasing cobalt concentrations in Sb_2S_3 thin films which might be due decrease in thickness of films which also shows reduction in crystallite size measured from XRD and particle size from SEM, similar cases were also reported in literature earlier [22]. This increased

absorbance (decreased transmittance) proved that these Co-doped Sb_2S_3 thin films will generate high photocurrent when used as

absorber layers in heterojunction thin film solar cells [10].

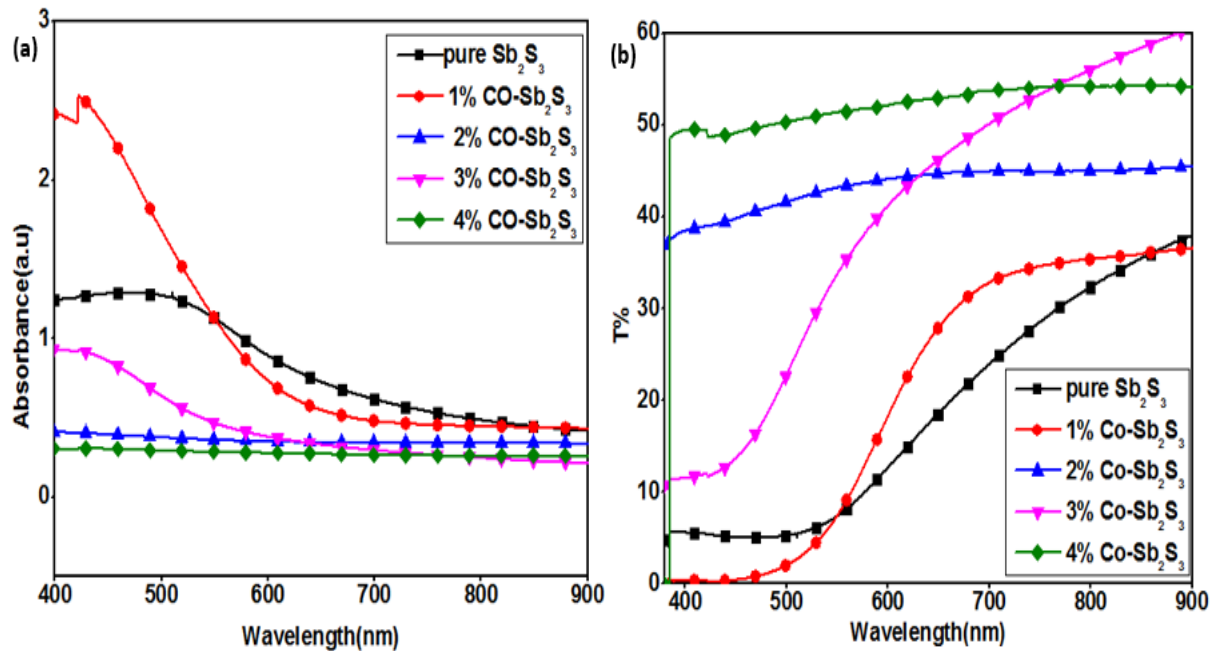


Figure 5 (a) Absorbance and (b) Transmittance of pure and Co-doped Sb_2S_3 thin films with 1%, 2%, 3% and 4% Co concentrations.

The absorption coefficient α for Co-doped Sb_2S_3 thin films was evaluated by transmittance using following relation [25]:

$$\alpha = \frac{1}{d} \ln\left(\frac{100}{T\%}\right) \quad (8)$$

Where d gives the film thickness. The plot of absorption coefficient α is shown in Fig. 6(a). The value of absorption coefficient has great impact on solar conversion efficiency. The pure and Co-doped Sb_2S_3 thin films have high absorption coefficient of the order of 10^4 cm^{-1}

$$n = \frac{1+\sqrt{R}}{1-\sqrt{R}}$$

Where R is reflectance of Co-doped Sb_2S_3 thin films which was calculated by $A+T+R=1$. The refractive index n , of cobalt doped Sb_2S_3 thin films is shown in Fig. 6(b). The energy band gap, refractive index and absorption coefficient of cobalt doped antimony sulphide thin films are compared in Table II. The refractive index decreases at higher wavelength for higher cobalt concentrations. It was found to be suitable as

ranges from 600 nm-900 nm which showed that material can be used as suitable candidate for absorber in solar cell applications [36].

The refractive index (n) for Co-doped Sb_2S_3 thin films was evaluated by given equation [34]:

$$(9)$$

good absorber applications and also may be suitable for use as an anti-reflection coating the same case was reported earlier in [37].

The crystallinity and smoothness of pure and Co-doped Sb_2S_3 thin films was found by extinction coefficient k , by formula given below [38]:

$$K = \frac{\alpha\lambda}{4\pi} \quad (10)$$

The wavelength versus extinction coefficient plot can be seen in Fig. 6(c). This plot shows that the value of extinction coefficient was higher at 400 nm-500 nm, which started to decrease from 600 nm-900 nm which showed compactness,

$$(\alpha h\nu)^n = A(h\nu - E_g) \quad (11)$$

where $n = 2, 1/2, 2/3$ depend on allowed direct-, allowed indirect-, and forbidden direct transitions respectively, A is constant, h is planks constant and α is absorption coefficient. The pure and Co-doped Sb_2S_3 thin films with varying cobalt concentrations have indirect band gap from 0.56 eV-0.95 eV which can be seen in Fig.7. This increasing pattern of band gap energy might be due to slight disruption of system and reduction in localized state density or phase variation due to higher cobalt concentrations. It has also been reported earlier that incorporation

crystallinity, levelness and uniformity of thin films.

The optical band gap energy value E_g of was cobalt doped Sb_2S_3 thin films measured by Tauc's equation:

of cobalt in chalcogenide materials increases band gap energy due to shifting of Fermi level. The chalcogenide thin films observed to have high defects doping of cobalt in Sb_2S_3 thin films decrease unsaturated defects which results in saturated bonds, might be the reason for increase in band gap energy [39, 40]. These bandgap energy values are given in Table II which supports literature [41] and also contribute to its use in large scale energy generation.

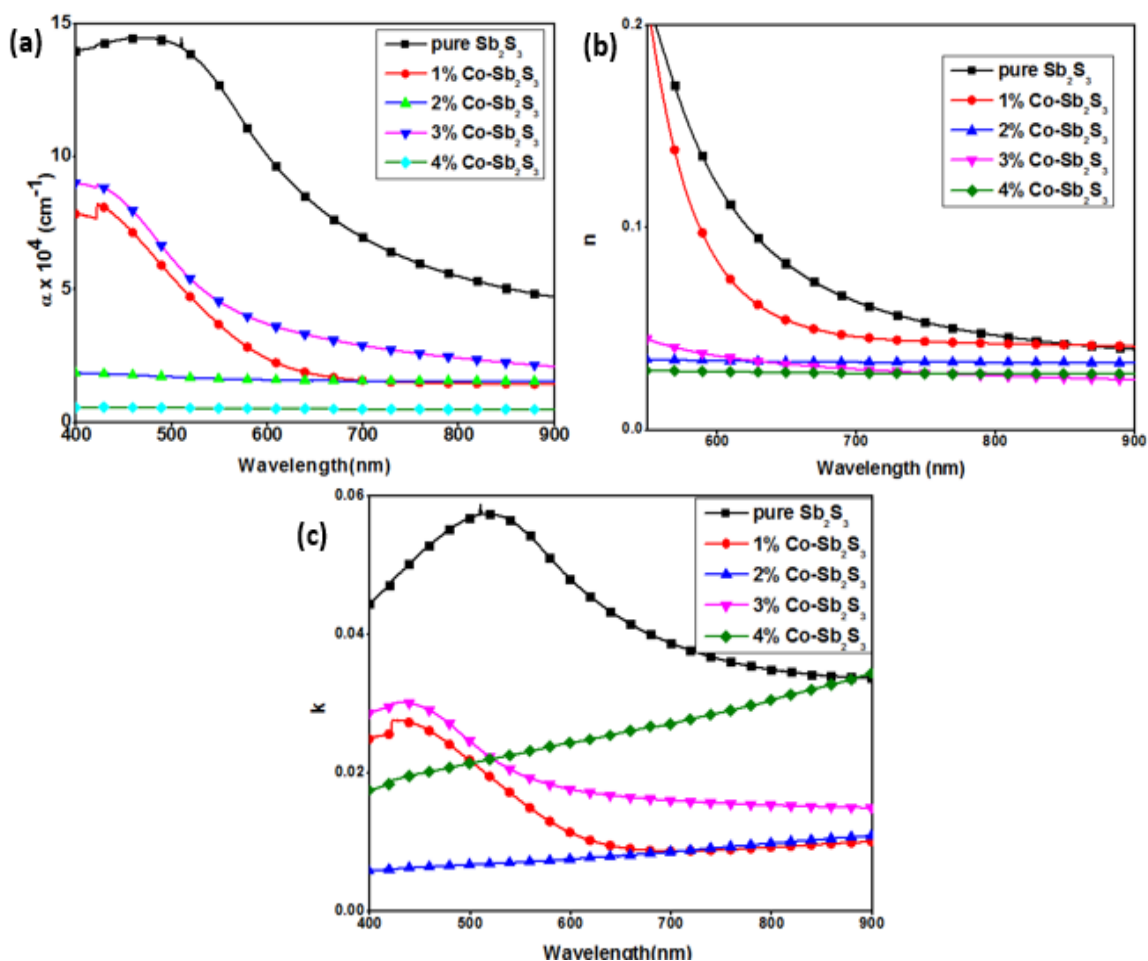


Figure 6. The plot (a) absorption coefficient α , (b) Refractive index n , (c) Extinction coefficient k of pure and cobalt doped Sb_2S_3 thin films with 1%,2%,3% and 4% Co concentrations.

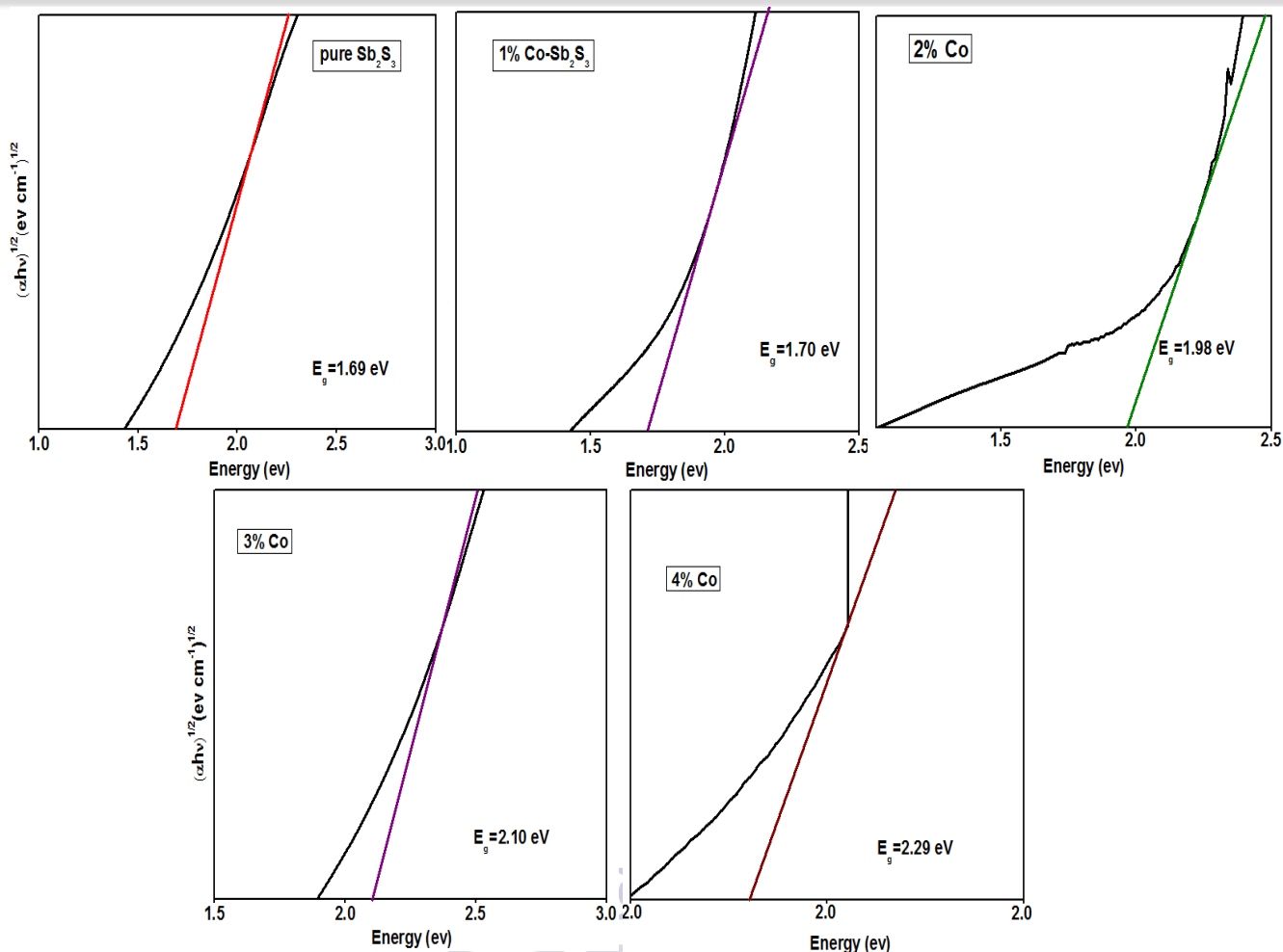


Figure 7. Bandgap energy values for pure and Co-doped Sb_2S_3 thin films.

Table II The comparison of optical parameters of Co-doped Sb_2S_3 thin films.

Sample	$E_g(\text{eV})$	$\alpha \times 10^4 \text{ cm}^{-1}$	n
Pure Sb_2S_3	1.69	10.21	0.19
1% Co- Sb_2S_3	1.70	6.82	0.11
2% Co- Sb_2S_3	1.98	1.85	0.03
3% Co- Sb_2S_3	2.10	8.35	0.04
4% Co- Sb_2S_3	2.19	0.53	0.02

4. Conclusion

To enhance the absorption and various structural and optical parameters of antimony sulphide thin films, Sb_2S_3 is doped by different cobalt concentrations. We have deposited the Co-doped Sb_2S_3 thin films by CBD technique optimized at low temperature of about 10^0 °C which was annealed at 250 °C. The prepared films were characterized by X-ray diffraction (XRD) from which we observe the structural parameters of thin films which showed that Co-doped Sb_2S_3 thin films were well covered and showed adhesive property of films. It was also

observed that films were polycrystalline in nature, their crystallite size decreased and dislocation density increased with increasing cobalt concentrations. The prepared films were also characterized by raman spectroscopy. The undoped and Co-doped Sb_2S_3 thin films were also observed by the characterization of scanning electron microscopy (SEM) which showed reduction in grain size and the particles become dense with increasing cobalt concentrations which showed compactness of films with uneven distribution of particles. These films were also characterized by UV/Visible spectroscopy from

which we observed that the films showed high absorbance in the range of 500 nm-900 nm and high transmittance of about 60 % in the wavelength ranges from 500 nm-900 nm can be seen for 3% cobalt concentration. The prepared pure and Co-doped Sb_2S_3 thin films were observed to have indirect band gap from 0.56 eV-0.95 eV, low refractive index and also have high absorption coefficient of the order of 10^4 cm^{-1} . It can be concluded from the above discussed structural, morphological and optical parameters that the cobalt-doped antimony sulfide thin films can be used as perfect material for optoelectronics as solar cell absorber material and can also be used as an anti-reflection coating.

Conflict of interest

The authors declare no conflict of interest.

REFERENCES

- Petkov, K., et al., *Changes in the physicochemical and optical properties of chalcogenide thin films from the systems As-S and As-S-Tl*. Journal of materials science, 2004. **39**(3): p. 961-968.
- Marquez, E., et al., *Optical properties and structure of amorphous (As_{0.33}S_{0.67})_{100-x}Te_x and GeSb_{40-x}S_{60-x} chalcogenide semiconducting alloy films deposited by vacuum thermal evaporation*. Journal of Physics D: Applied Physics, 2006. **39**(9): p. 1793.
- Zhang, H., et al., *Synthesis of 1D Sb₂S₃ nanostructures and its application in visible-light-driven photodegradation for MO*. Journal of Alloys and Compounds, 2015. **625**: p. 90-94.
- Ghrairi, N., et al., *Comparative studies of the properties of thermal annealed Sb₂S₃ thin films*. Chalcogenide Letters, 2010. **7**(3): p. 217-225.
- Nair, M., et al., *Chemically deposited Sb₂S₃ and Sb₂S₃-CuS thin films*. Journal of the Electrochemical Society, 1998. **145**(6): p. 2113.
- Aousgi, F. and M. Kanzari, *Study of the optical properties of the amorphous Sb₂S₃ thin films*. Journal of Optoelectronics and Advanced materials, 2010. **12**(2): p. 227.
- Ali, N., et al., *200° C annealed combinatorially deposited chalcogenide based metallic thin films for photovoltaics*. Measurement, 2015. **63**: p. 81-86.
- Calixto-Rodriguez, M., et al. *AC plasma induced modifications in Sb₂S₃ thin films*. in Journal of Physics: Conference Series. 2010. IOP Publishing.
- Versavel, M.Y. and J.A. Haber, *Lead antimony sulfides as potential solar absorbers for thin film solar cells*. Thin Solid Films, 2007. **515**(15): p. 5767-5770.
- Mushtaq, S., et al., *Low-temperature synthesis and characterization of Sn-doped Sb₂S₃ thin film for solar cell applications*. Journal of Alloys and Compounds, 2015. **632**: p. 723-728.
- Yesugade, N., C. Lokhande, and C. Bhosale, *Structural and optical properties of electrodeposited Bi₂S₃, Sb₂S₃ and As₂S₃ thin films*. Thin Solid Films, 1995. **263**(2): p. 145-149.
- Rajpure, K., C. Lokhande, and C. Bhosale, *A comparative study of concentration effect of complexing agent on the properties of spray deposited Sb₂S₃ thin films and precipitated powders*. Materials chemistry and physics, 1997. **51**(3): p. 252-257.
- Abd-El-Rahman, K. and A. Darwish, *Fabrication and electrical characterization of p-Sb₂S₃/n-Si heterojunctions for solar cells application*. Current Applied Physics, 2011. **11**(6): p. 1265-1268.
- Nayak, B., et al., *The dip-dry technique for preparing photosensitive Sb₂S₃ films*. Thin Solid Films, 1982. **92**(4): p. 309-314.
- Aousgi, F. and M. Kanzari, *Study of the optical properties of Sn-doped Sb₂S₃ thin films*. Energy Procedia, 2011. **10**: p. 313-322.
- Cárdenas, E., et al., *Carbon-doped Sb₂S₃ thin films: structural, optical and electrical properties*. Solar energy materials and solar cells, 2009. **93**(1): p. 33-36.

- Nwofe, P., P. Agbo, and C. Ozibo, COMPOSITIONAL AND OPTICAL ANALYSIS OF CHEMICALLY DEPOSITED ZINC-DOPED ANTIMONY SULPHIDE THIN FILMS. Chalcogenide Letters, 2016. 13(10).
- Lokhande, C., et al., XRD, SEM, AFM, HRTEM, EDAX and RBS studies of chemically deposited Sb₂S₃ and Sb₂Se₃ thin films. Applied surface science, 2002. 193(1-4): p. 1-10.
- Salem, A. and M.S. Selim, Structure and optical properties of chemically deposited Sb₂S₃ thin films. Journal of Physics D: Applied Physics, 2001. 34(1): p. 12.
- Savadogo, O. and K. Mandal, Low Cost Schottky Barrier Solar Cells Fabricated on CdSe and Sb₂S₃ Films Chemically Deposited with Silicotungstic Acid. Journal of the Electrochemical Society, 1994. 141(10): p. 2871.
- Messina, S., M. Nair, and P. Nair, Antimony sulfide thin films in chemically deposited thin film photovoltaic cells. Thin Solid Films, 2007. 515(15): p. 5777-5782.
- Akata Nwofe, P. and M. Sugiyama, Microstructural, optical, and electrical properties of chemically deposited tin antimony sulfide thin films for use in optoelectronic devices. physica status solidi (a), 2020. 217(9): p. 1900881.
- Bennaji, N., et al., Thermal, Electrical and Dielectric Characteristics of SnSbS Thin Films for Solar Cell Applications. Journal of Electronic Materials, 2020. 49(2): p. 1354-1361.
- Cerdán-Pasarán, A., et al., Effect of cobalt doping on the device properties of Sb₂S₃-sensitized TiO₂ solar cells. 2019. 183: p. 697-703.
- Abdin, Z., et al., EFFECT OF Fe DOPANT ON PHYSICAL PROPERTIES OF ANTIMONY SULPHIDE (Sb₂S₃) THIN FILMS. Chalcogenide Letters, 2019. 16(1).
- Kosa, T., et al., Nonlinear optical properties of silver-doped As₂S₃. Journal of non-crystalline solids, 1993. 164: p. 1219-1222.
- Wang, X., et al., Luminescence and Raman scattering properties of Ag-doped ZnO films. Journal of Physics D: Applied Physics, 2006. 39(23): p. 4992.
- Maghraoui-Meherzi, H., et al., Structural, morphology and optical properties of chemically deposited Sb₂S₃ thin films. Physica B: Condensed Matter, 2010. 405(15): p. 3101-3105.
- Dong, D., et al., In situ "clickable" zwitterionic starch-based hydrogel for 3D cell encapsulation. ACS applied materials & interfaces, 2016. 8(7): p. 4442-4455.
- Eensalu, J.S., et al., Uniform Sb₂S₃ optical coatings by chemical spray method. Beilstein journal of nanotechnology, 2019. 10(1): p. 198-210.
- Osuwa, J. and R. Osuji, ANALYSIS OF ELECTRICAL AND MICRO-STRUCTURAL PROPERTIES OF ANNEALED ANTIMONY SULPHIDE (Sb₂S₃) THIN FILMS. Chalcogenide Letters, 2011. 8(9): p. 571-577.
- Diliegros-Godines, C., et al., Effect of Ag doping on structural, optical and electrical properties of antimony sulfide thin films. 2018. 53(16): p. 11562-11573.
- Mushtaq, S., et al., Nickel antimony sulphide thin films for solar cell application: study of optical constants. Natural Science, 2016. 8(2): p. 33-40.
- Ismail, B., S. Mushtaq, and A. Khan, Enhanced grain growth in the Sn doped Sb₂S₃ thin film absorber materials for solar cell applications. Chalcogenide Letters, 2014. 11(1): p. 37-45.
- Tarey, R.D. and T. Raju, A method for the deposition of transparent conducting thin films of tin oxide. Thin Solid Films, 1985. 128(3-4): p. 181-189.
- Ghraïri, N., et al., Comparative studies of the properties of thermal annealed Sb₂S₃ thin films. 2010. 7(3): p. 217-225.
- Onyia, A., Optical characteristics of co-deposited zinc antimony sulphide thin films. MDC J, 2017. 4: p. 159-169.

Priya, D.C., et al., *Thermally Deposited Sb₂S₃: Bi Thin Films for Solar Cell Absorber*. Journal of New Materials for Electrochemical Systems, 2018. **21**(1): p. 037-042.

Ubale, A., et al., *ELECTRICAL, OPTICAL AND STRUCTURAL PROPERTIES OF NANOSTRUCTURED Sb₂S₃ THIN FILMS DEPOSITED BY CBD TECHNIQUE*. Chalcogenide Letters, 2010. **7**(1): p. 101-109.

Syed, W., et al., *STRUCTURAL AND OPTICAL INVESTIGATION OF COBALT DOPED SnSb₂S₄ THIN FILMS FOR PHOTOVOLTAIC APPLICATIONS*. 2017. **14**(7): p. 259-265.

Radzwan, A., et al., *Ab initio calculations of optoelectronic properties of antimony sulfide nano-thin film for solar cell applications*. Results in Physics, 2019. **15**: p. 102762.

